Urinary Bladder Volume Reconstruction Based on Bioimpedance Measurements: Ex Vivo and In Vivo Validation Through Implanted Patch and Needle Electrodes

Federica Semproni, *Graduate Student Member, IEEE*, Veronica Iacovacci, *Member, IEEE*, Stefania Musco, and Arianna Menciassi, *Fellow, IEEE*

***Abstract*—Restoring bladder sensation in patients with bladder dysfunctions by performing urinary volume monitoring is an ambitious goal. The bioimpedance technique has shown promising results in wearable solutions but long-term validation and implantable systems are not available, yet. In this work, we propose to implant commercial bioimpedance sensors on bladder walls to perform bladder volume estimation. Two commercial sensor types (Ag/AgCl patch and needle electrodes) were selected for this purpose. An injected current frequency of 1.337 MHz and electrodes paired on the same face of the bladder allowed us to correlate the changes in impedance with increasing volumes. Two volume reconstruction algorithms have been proposed, based on the direct correlation between bioimpedance readings and bladder volume (Algorithm A) or bioimpedance readings and inter-electrode distance (Algorithm B, bladder shape approximated to a sphere). For both algorithms, a better fit with a second-degree fitting polynomial was obtained. Algorithm A obtained lower estimation errors with an average of 20.35% and 21.98% (volumes greater than 150 mL) for patch and needle electrodes, respectively. The variations in ion concentration led to a slight deterioration of volume estimation; however, the presence of tissues surrounding the bladder did not influence the performance. Although Algorithm B was less affected by the experimental conditions and inter-subject biological variability, it featured higher estimation errors. In vivo validation on the supine model showed average errors of 29.36% (volumes greater than 100 mL), demonstrating the potential of the proposed solution and paving the way toward a novel implantable volume monitoring system.**

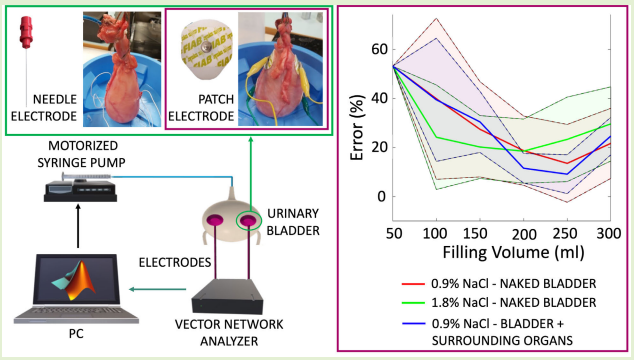

***Index Terms*— Bioimpedance, bladder volume monitoring, implantable biorobotic organs, implantable sensors.**

Manuscript received 18 September 2023; accepted 26 October 2023. Date of publication 14 November 2023; date of current version 14 December 2023. This work was supported by the Istituto nazionale Assicurazione Infortuni sul Lavoro (INAIL), the Italian National Institute for Insurance against Work-related Injuries (non-commercial entity), within the PR19-CR-P2 BioSUP (BIOnic Solutions for Urinary impaired People) Project Framework. The associate editor coordinating the review of this article and approving it for publication was Dr. Yang Yang. *(Corresponding author: Federica Semproni.)*

This work involved human subjects or animals in its research. Approval of all ethical and experimental procedures and protocols was granted by the Italian Ministry of Health (Authorization n° 278/2021-PR in response to application n.65E5B.65), and performed in line with the Italian Law (D.lgs. 26/2014).

Federica Semproni, Veronica Iacovacci, and Arianna Menciassi are with the BioRobotics Institute, Scuola Superiore Sant'Anna, 56025 Pisa, Italy (e-mail: federica.semproni@santannapisa.it; veronica.iacovacci@santannapisa.it; arianna.menciassi@santannapisa.it).

Stefania Musco is with the Neuro-Urology of Azienda Ospedaliero Universitaria Careggi, 50139 Florence, Italy (e-mail: stefaniamusco@gmail.com).

This article has supplementary downloadable material available at https://doi.org/10.1109/JSEN.2023.3330978, provided by the authors.

Digital Object Identifier 10.1109/JSEN.2023.3330978

I. Introduction

BLADDER filling and emptying are regulated by the interplay between the lower urinary system organs (the urinary bladder, the detrusor muscle, the sphincters, and the urethra) and the nervous system [1]. Bladder filling state sensation depends on stretch receptors positioned on the bladder wall and sending afferent sensory signals to the brain. In healthy people, the first need to void is perceived when bladder urine volume reaches 250–300 mL and it becomes stronger close to the maximum bladder capacity (i.e., 400–600 mL) [2].

Neurological and neurodegenerative pathologies can impair bladder sensory feedback [3]. Bladder sensation dysfunctions affect millions of people producing discomfort and threatening autonomous micturition. In this framework, there is a real need for solutions to support bladder volume monitoring for patient-aware urination management.

Several diagnostic imaging and sensing techniques have been proposed for bladder volume estimation through clinical or wearable devices [4]. In this scenario, bioimpedance-based

monitoring proved promising since it requires easy-to-apply and light-weighted electrodes and simple driving electronics, it has no stringent requirements in electrode positioning, and it allows for continuous and operator-independent measurements. Bioimpedance also features a strong relationship with urine volume [5]. Bioimpedance-based monitoring proved efficient in wearable devices and in different biomedical applications, such as blood perfusion and gastroesophageal reflux evaluation through implantable sensors [6], [7], [8], [9].

However, relying on wearable and sometimes bulky monitoring systems prevents chronic use and the reliable combination of the monitoring system with a urinary assistive device or prosthesis. Bioimpedance measurements have never been implemented in implantable systems for bladder volume monitoring, so far. Resistive and capacitive stretchable sensors have been proposed as implantable solutions to correlate bladder deformation with its filling state [10], [11], [12]. However, the nonoptimal mechanical compliance between the sensor and the bladder tissue either prevents the natural behavior of the bladder or determines monitoring artifacts. Furthermore, correlating tissue deformation and volume variation is not straightforward and a multisensors system should be considered to track the anisotropic expansion and contraction of the bladder.

In this framework, we propose a novel approach with the twofold objective to overcome the limitations shown by state-of-the-art implantable bladder monitoring systems and to prove the feasibility of implanting electrodes for bioimpedance-based bladder volume estimation. To this aim, we compared two classes of commercial electrodes when varying the operating frequency and sensor position on the bladder. Dedicated volume estimation algorithms based on bioimpedance measurements were developed and validated through ex vivo tests. A set of operating parameters (e.g., electrode position and working frequency) allowing volume estimation error minimization was identified and preliminarily validated in vivo on the suine model. In vivo test results confirmed those obtained ex vivo paving the way to the development of implantable volume monitoring systems based on bioimpedance measurements.

II. Materials and Methods

Urine volume changes in the bladder produce impedance variations that can be recorded and correlated with bladder volume. The impedance (Z) can be defined as follows:

$$Z = R + iX \tag{1}$$

where R is the resistive component (resistance) and X is the imaginary reactive component (reactance). The bioimpedance variations in the urinary bladder can be recorded through dedicated electrodes. The minimum number of electrodes to be employed is two (bipolar measure): one electrode is used to inject a small alternating current (in the range of μA–mA) in the tissue, whereas a second one is used to read the voltage-induced at a certain distance from the injecting electrode [see Fig. 1(a)].

Configurations employing more than two electrodes (e.g., tetrapolar measure) have been reported in the literature to reduce the influence of cable resistance and electrode-skin impedance [13]. However, given the reduced space in the abdominal cavity, by tightly suturing the electrodes to the bladder wall, bladder-electrode reciprocal movements can be limited together with the associated artifacts [14]. Electrodes suturing can justify the use of bipolar measurements which permits in turn to use of smaller and simpler electronics. In addition, preliminary tests demonstrated that traditional tetrapolar measurements did not significantly improve the quality of the data, so we used bipolar measurements.

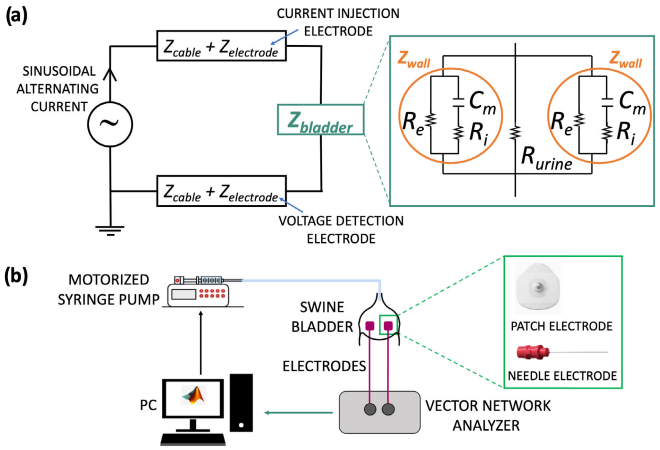

Fig. 1. Bioimpedance-based bladder volume estimation. (a) Bipolar bladder impedance measurement equivalent circuit. Bladder wall (Z_{wall}) and urine (R_{urine}) contributions are considered. Tissue walls are schematized as a parallel of two equivalent circuits, with two resistive components (R_e and R_i) and a capacitive component (C_m). (b) Experimental setup used for ex vivo tests.

Considering the path of the current between the injection and detection electrodes [see Fig. 1(a)], the bladder bioimpedance ($Z_{bladder}$) results from the superposition of the urine and the bladder wall contributions.

Bladder walls can be represented with the parallel of two equivalent circuits each including the resistive components of extracellular (R_e) and intracellular (R_i) fluids as well as the capacitive component of cell membranes (C_m) [15].

While the bladder walls component of impedance slightly varies with the filling level, the component associated with urine strongly depends on it. This is particularly true for R_{urine} which depends on the urine volume (direct proportionality) and conductivity (indirect proportionality) [13].

In this article, the authors aim to correlate bladder bioimpedance variations recorded through implantable electrodes with the volume of urine collected in the bladder. In this direction, to shed light on the role played by electrode dimension and position with respect to tissue, superficial Ag/AgCl patch electrodes (dimensions: 36 × 45 mm)–generally used for echocardiography–and needle electrodes [dimensions: 30 mm (length) × 0.35 mm (diameter)]–generally used for the collection of intramuscular signals–were compared [see Fig. 1(b)]. The first electrode type represents the gold standard for bioimpedance signal recording in wearable systems as they are easy to apply on tissues. The second type of electrodes was selected to investigate whether surrounding organs still influence bladder bioimpedance when placing the electrodes across the organ walls tissue.

Fig. 2 shows the workflow followed in this article to systematically compare the two electrode types and to identify

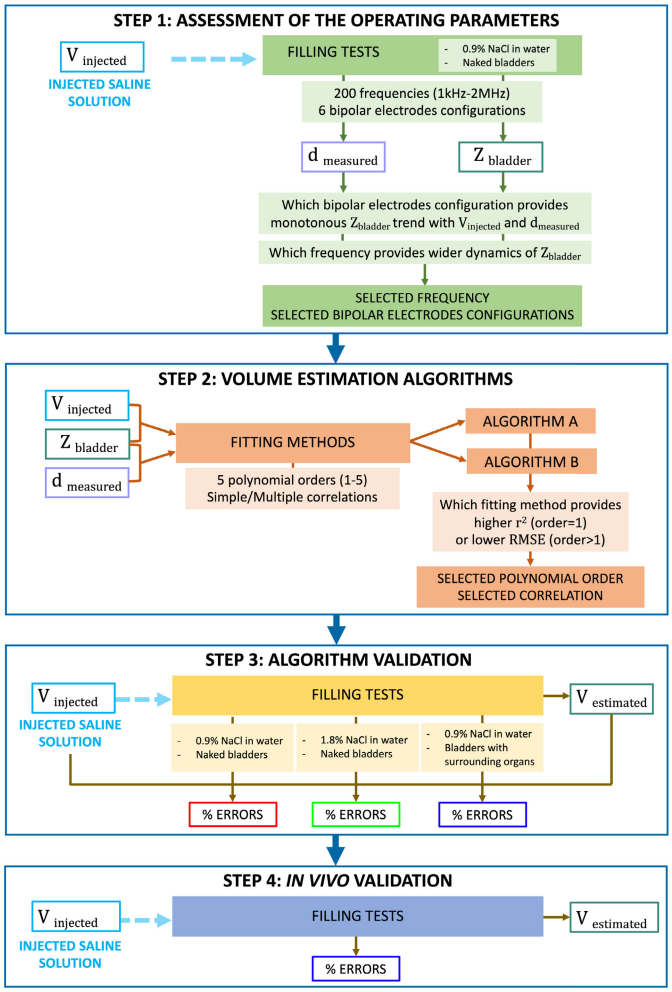

Fig. 2. Article workflow to compare the two types of electrodes and select the volume estimation algorithms. Step 1) Assessment of the operating parameters (bipolar electrode configuration and working frequency) under standard conditions. Step 2) Volume estimation algorithms based on fitting methods to define the polynomial order and the correlation type. Step 3) Validation of algorithms by comparing estimation errors under standard experimental conditions and in more realistic experimental conditions. Step 4) In vivo validation.

both the working conditions and the best volume estimation algorithm.

First, ex vivo experiments on swine bladders were performed under standard experimental conditions (bladders without surrounding organs, called "naked bladders" in this article, filled with a saline solution to simulate the average ion concentration of human urine–0.9% NaCl in water–in physiological conditions [16]). The injected current frequency and the bipolar configuration of electrodes were varied to identify the optimal working conditions, which provide a monotonous trend and wide dynamics of impedance components with increasing filling volumes and consequent increase in distance between the electrodes d_{measured} (Step 1, Fig. 2). Subsequently, volume estimation was performed through two dedicated algorithms, using the recorded impedance and inter-electrodes distance values as inputs, respectively (Step 2, Fig. 2). Different fitting methods and polynomial orders were compared to define the condition for minimizing the volume estimation errors. To assess the feasibility of the proposed approach in bladder monitoring, the performances of the volume estimation algorithms were validated ex vivo on swine bladders in more realistic experimental conditions while varying the urine conductivity and adding tissues surrounding the bladders (Step 3, Fig. 2), and in vivo (Step 4, Fig. 2).

A. Experimental Setup

The same experimental setup [see Fig. 1(b)] was used for all the ex vivo experiments. It includes two electrodes (either patch or needle type), a vector network analyzer (model DG8SAQ VNWA v3, SDR-Kits, frequency range 1 kHz–1.3 GHz) for impedance recording, and a motorized syringe pump (New Era NE-1000 Multiphaser Programmable Syringe Pump) for controlled bladder filling. The network analyzer allows to variation of the working frequency and to recording of impedance data as complex numbers, thus distinguishing the resistive and the reactive components. Porcine bladders were used to carry out the tests and were positioned vertically with the urethra upward to facilitate filling and prevent leakage, while the ureters were kept closed by collapsing. Bladders of approximately the same size were gradually filled from the urethra starting from the empty status (0 mL) till reaching the full status (300 mL, simulating human bladder volume of the first need to void) through 50 mL steps. Cyanoacrylate-based glue (together with tight sutures) was used to attach the nonconductive part of the electrodes to the external walls of the bladders. Inter-electrode distance measurements (d_{measured} in cm) were performed by a twine thread placed on the bladder to connect the two electrode centers. These distances were used in the volume estimation phase.

B. Assessment of the Operating Parameters (STEP 1)

As a first step, we aimed to identify which bipolar configuration and working frequency provide monotonous trends and wide dynamics of impedance components with increasing filling volumes.

Ex vivo filling tests on nine swine bladders were performed under standard experimental conditions to evaluate Z_{bladder} and d_{measured} values (Step 1 in Fig. 2). Filling tests were repeated varying the bipolar configuration of electrodes (see Fig. 3) and the injected current frequency.

Despite the symmetry in vertical and cross-configurations (3–4 and 5–6), all the six identified configurations were tested to account for the anisotropic expansion of the bladder during filling [17].

Z_{bladder} readings were carried out over 200 frequencies in the range 1 kHz–2 MHz, i.e., the range of frequencies typically used for tissue analysis [6]. In fact, at lower frequencies, the current does not penetrate the cell membranes [schematized with C_m in Fig. 1(a)] which behave like open circuits making the current flow only through the extracellular fluids (R_e). At higher frequencies, the cell membranes will behave as short circuits and the current will flow both through the intracellular (R_i) and extracellular fluids (R_e). The 200 frequencies were grouped into three ranges, namely, low, medium, and high, and the trend of the data for each range was analyzed. For each bladder, the resistive and the reactive components of impedance were read by the network analyzer.

C. Volume Estimation Algorithms (STEP 2)

The impedance data recorded at different working frequencies and bipolar electrode configurations were used to identify

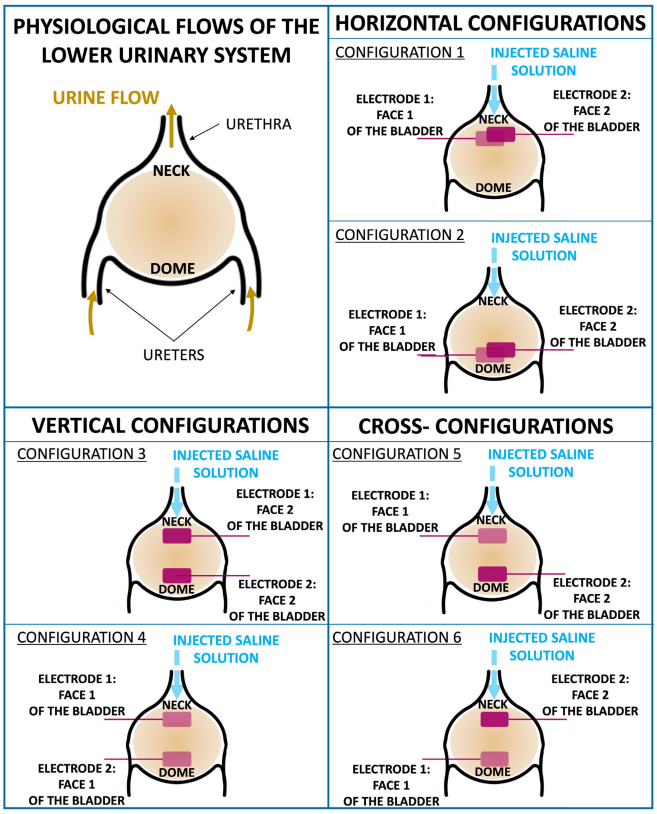

Fig. 3. Representation of the investigated electrodes' bipolar configurations. The configurations are classified as: horizontal (1 and 2); vertical (3 and 4); and cross (5 and 6). The bladders are vertically oriented, and the arrows represent the physiological flow of urine (in ocher) and the flow of saline solution (in light blue). The bladder walls are named face 1 and face 2.

a fitting law correlating bioimpedance and internal bladder volume (Algorithm A) or inter-electrode distance (Algorithm B).

The impedance read by the vector network analyzer, the inter-electrodes distance measurements, and the injected volume data were imported into the MathWorks environment (MATLAB R2020b version) for analysis. To read the complex impedance measurements from the single-port touchstone files of the network analyzer (".s1p" format), the radio frequency toolbox (*zparameters* and *rfparameters* functions) was used.

High impedance variability was witnessed among the different bladders when considering the first part of the filling range (below 50 mL). To make the algorithm robust to intra-subject biological variability, data were scaled with respect to the impedance value recorded at 50 mL of filling (to remove the bladder wall contribution), and all the data processing steps were performed on bioimpedance delta ($\Delta Z_{\text{bladder}}(i)$) defined as follows:

$$\Delta Z_{\text{bladder}}(i) = Z_{\text{bladder}}(i) - Z_{\text{bladder}}(50\ \text{mL}) \quad (2)$$

$$\Delta Z_{\text{bladder}} = \Delta R_{\text{bladder}} + i\Delta X_{\text{bladder}} \quad (3)$$

where $Z_{\text{bladder}}(i)$ represents the impedance readings at ith filling volume, Z_{bladder} (50 mL) represents the impedance readings at 50 mL of urine volume, $\Delta R_{\text{bladder}}$ and $\Delta X_{\text{bladder}}$ represent the scaled resistive and reactive components of impedance. Since the measurements are evaluated as

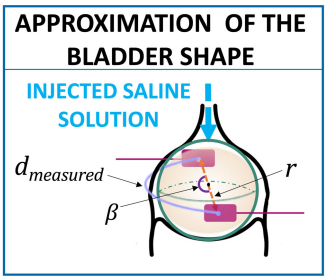

Fig. 4. Bladder shape approximation to a sphere. d_{measured} is the length of the arc of circumference manually taken by a twine thread placed on the bladder to connect the two electrode centers during the ex vivo tests. The sphere radius r of the sphere is derived from d_{measured} and the central angle (ß).

impedance variations, the electrode impedance ($Z_{\text{cable}} + Z_{\text{electrode}}$) can be considered negligible.

Two volume estimation algorithms were developed (Step 2 in Fig. 2). In the first case (Algorithm A), a direct correlation between bioimpedance readings and bladder volume (V_{injected}) was derived. In the latter (Algorithm B), bioimpedance was correlated to inter-electrodes distance (d_{measured}), and urinary volume was estimated by approximating the bladder shape to a sphere (see Fig. 4) (for other shape approximations the reader is redirected to the Supplementary Material). In this regard, the sphere radius (r in Fig. 4) was derived from d_{measured} (and assuming ß 180° for configurations 1–2–5–6, and 120° for configurations 3–4). In both cases, fitting methods with various polynomial orders (from 1 to 5) were used to perform simple correlations (i.e., between $\Delta R_{\text{bladder}}$–$V_{\text{injected}}$ and $\Delta X_{\text{bladder}}$–$V_{\text{injected}}$ in Algorithm A and between $\Delta R_{\text{bladder}}$–$d_{\text{measured}}$ and $\Delta X_{\text{bladder}}$–$d_{\text{measured}}$ in Algorithm B) and multiple regressions (i.e., between $\Delta R_{\text{bladder}}$–$\Delta X_{\text{bladder}}$–$V_{\text{injected}}$ in Algorithm A and between $\Delta R_{\text{bladder}}$–$\Delta X_{\text{bladder}}$–$d_{\text{measured}}$ in Algorithm B). Two statistical parameters were calculated to help identify the best fitting polynomial: the coefficient of determination (r^2) to evaluate the goodness of the first-order fitting polynomial and the root mean square error (RMSE) to evaluate the goodness of the fitting polynomials with order higher than 1.

D. Algorithms Validation (STEP 3)

The capability of the two algorithms to predict the bladder volume was evaluated by comparing the estimated volume ($V_{\text{estimated}}$) with the injected one (V_{injected}). In this sense, the estimation errors obtained under standard conditions were evaluated against the errors obtained in a more realistic operating scenario (Step 3 in Fig. 2).

To this aim, filling tests were repeated (for the selected bipolar configuration and working frequency) to take into account the influence on bioimpedance of urine composition (i.e., ion concentration), and organs surrounding the bladder.

To evaluate the first condition, tests were performed on three swine bladders gradually filled with saline solution at high concentrations, i.e., 1.8% NaCl in water (the maximum ion concentration of human urine in pathological conditions [18]).

Three additional swine bladders were used to test the second condition, thus the presence of other organs in contact with the urinary bladder. The influence of organs was referred to as electrical properties and not spatial encumbrance. The bladders were gradually filled with saline solution (0.9% NaCl in water)

and additional porcine tissue was placed around the bladder during the experiments.

E. In Vivo Validation (STEP 4)

To validate the use of bioimpedance sensors to monitor bladder volume in an implantable setting, we performed a preliminary in vivo test on a female pig bladder (protocol 65E5B.6, 25 kg farm pig).

After the pig was placed in the supine position, an abdominal midline incision was made to expose the urinary bladder. A 6-F catheter was inserted into the bladder through the urethra for bladder filling, and the selected electrodes were sutured (2/0 Vicryl) on the bladder walls in the selected configuration (electrode type and configuration providing the best outcomes ex vivo were employed in the in vivo tests). The bladder was inserted in the abdomen and the incision was closed with surgical thread. The bladder was gradually filled in situ from 0 mL to the anesthetic capacity (250 mL) with a constant filling rate of 30 mL/min using a cystometric pump, and $\Delta R_{\text{bladder}}$ and $\Delta X_{\text{bladder}}$ values recorded with the vector network analyzer, already used for the ex vivo tests. During filling intravenous fluid was stopped to restrict the physiological diuresis. The bladder was manually voided with a syringe through the urethra, and bladder filling was repeated three times in the same way.

Data were imported and analyzed in the MathWorks environment. Considering that the conductivity of in vivo tissues is higher than ex vivo ones, we applied a correction factor allowing to use of the same algorithm obtained from ex vivo data fitting [19], [20]. Furthermore, a large inter-subject biological variability was observed during the experiments among the ex vivo and in vivo animals (a strong component of bladder capacity variability due to the animal's habits still exists). For this reason, the impedance data were related to the percentage of filling (0 mL corresponds to 0%, and volume to capacity corresponds to 100%).

Finally, bladder filling volumes were estimated using the optimal algorithm identified in Step 3.

III. Results and Discussion

A. Definition of the Operating Parameters

Ex vivo tests performed over bladder filling cycles under standard experimental conditions allowed us to select the operating parameters to obtain an optimal correlation between bioimpedance and volume or inter-electrode distance.

We focused the analysis on the variation of $\Delta X_{\text{bladder}}$ which is more sensitive to frequency (see Figs. S2 and S3). The electrode configurations featuring an increasing monotonous trend of $\Delta X_{\text{bladder}}$ with volume were preferred. This led to discard configurations 1 (for patch electrodes) and 2 (for both electrodes) in the following analysis. This could have been derived also intuitively given that the electrodes are both too close or too far from the inlets (even if we consider the upside-down configuration exploited during experiments) to properly follow filling dynamics.

From the working frequency range viewpoint, the one featuring wider dynamics over the tested volume range was selected (see Figs. S2 and S3). Indeed, larger impedance dynamics allow us to better correlate the changes in impedance with increasing volumes. Frequencies of the lowest analyzed range produced minor variations of $\Delta X_{\text{bladder}}$ with volume (and also not increasing trend for needle electrodes) for all the tested configurations. High-range frequencies proved preferable for patch electrodes whereas larger dynamics, higher repeatability, and monotonous trend were observed with needle electrodes driven with mid-range frequencies.

To mediate between the different behaviors while looking for a single working frequency allowing to perform a comparative analysis of the two electrode types, 1.337 MHz (halfway between the two ranges) was selected for further investigations.

In addition, no significant difference was witnessed among symmetrical configurations (3–4 and 5–6), (see Tables SI and SII). For these reasons, configurations 4 and 6 were not tested further. For more details, the reader is redirected to the Supplementary Material.

TABLE I

r^2 AND RMSE (mL) VALUES OF THE FITTING METHODS USED TO ESTIMATE THE BLADDER VOLUME FROM $\Delta R_{\text{BLADDER}}$ AND $\Delta X_{\text{BLADDER}}$ (ALGORITHM A) ARE REPORTED FOR THE TWO SELECTED CONFIGURATIONS, FOR BOTH ELECTRODE TYPES. RESULTS FOR DIFFERENT POLYNOMIAL DEGREES ARE REPORTED (1–2–5)

ALGORITHM A						
PATCH ELECTRODES						
	CONFIGURATION 3			**CONFIGURATION 5**		
Statistical Parameter	**r^2**	**RMSE (ml)**		**r^2**	**RMSE (ml)**	
Polynomial Order	**1**	**2**	**5**	**1**	**2**	**5**
$\Delta R_{\text{bladder}}$ - d_{measured}	0.54	54.30	52.37	0.46	56.59	53.79
$\Delta X_{\text{bladder}}$ - d_{measured}	0.39	138.10	138.56	0.30	136.87	136.17
$\Delta R_{\text{bladder}}$ - $\Delta X_{\text{bladder}}$ - d_{measured}	0.60	53.94	50.68	0.56	55.89	52.37
NEEDLE ELECTRODES						
	CONFIGURATION 3			**CONFIGURATION 5**		
Statistical Parameter	**r^2**	**RMSE (ml)**		**r^2**	**RMSE (ml)**	
Polynomial Order	**1**	**2**	**5**	**1**	**2**	**5**
$\Delta R_{\text{bladder}}$ - d_{measured}	0.15	78.59	75.44	0.13	78.68	76.64
$\Delta X_{\text{bladder}}$ - d_{measured}	0.13	101.67	104.59	0.32	102.17	106.21
$\Delta R_{\text{bladder}}$ - $\Delta X_{\text{bladder}}$ -d_{measured}	0.46	60.43	51.71	0.34	66.29	62.59

B. Choice and Testing of the Fitting Model

We proceeded by implementing two algorithms to estimate the bladder volume based on the selected working frequency (i.e., 1.337 MHz) and the electrode configurations (i.e., 3–5) featuring wider dynamics and monotonous trend of impedance components over the tested volume range. $\Delta R_{\text{bladder}}$ and $\Delta X_{\text{bladder}}$ were provided as input to the algorithms, either as single components to evaluate the respective influence in volume estimation, or in combination.

1) Algorithm A: Linear statistical models did not correctly predict the values of the dependent variable V_{injected} starting from bioimpedance data. This behavior was witnessed for both the configurations (3 and 5) and both electrode types (see Table I), resulting in a coefficient of determination r^2 always significantly lower than 1, for both $\Delta R_{\text{bladder}}$ and $\Delta X_{\text{bladder}}$. Simple correlations were better performed in estimating the volume starting from $\Delta R_{\text{bladder}}$ for both electrode types–as R_{urine} plays a fundamental role–but featured high RMSE (around 50 and 75 mL for patch and needle electrodes, respectively).

RMSE values decreased when using multiple regressions for needle electrodes. Increasing the degree of the fitting polynomial from 2 to 5 did not lead to an improvement in the prediction of volumes in terms of RMSE values (for RMSE values obtained with 3° and 4° the reader is redirected to the Supplementary Material, Table SIII). Therefore, a second-degree polynomial-based multiple regression model was selected for further analysis, for both electrode types. Given that no major differences emerged between the two selected bipolar configurations, we decided to proceed only with configuration 3 which would favor future implantation and connection to the reading unit due to the placement of the electrodes on the same bladder face.

Based on the considerations above, we proceeded by estimating bladder volume starting from both values of $\Delta R_{\text{bladder}}$ and $\Delta X_{\text{bladder}}$ through a second-degree fitting polynomial for both electrode types.

2) Algorithm B: As for the previous algorithm, for both electrode types and configurations, the linear statistical models did not correctly predict the values of the dependent variable d_{measured} (r^2 values much lower than 1). No significant differences in RMSE values were reported among simple correlations and multiple regressions, not even between the two types of electrodes (see Table II). The reader is redirected to the Supplementary Material for RMSE values obtained with 3° and 4° (see Table SIV).

However, the bipolar configuration 3 allowed for a better estimate of the inter-electrode distances $d_{\text{estimated}}$ (lower RMSE). Furthermore, no improvements in fitting were found by increasing the degree of the polynomial. For these reasons, we decided to proceed by estimating the inter-electrodes distance from both values of $\Delta R_{\text{bladder}}$ and $\Delta X_{\text{bladder}}$ and using the multiple second-degree polynomial and configuration 3 for both electrode types.

C. Volume Estimation and Algorithms Validation in Different Experimental Conditions

Volume estimation performance was tested both under standard experimental conditions and in unpredictable conditions that might occur in vivo. This allowed us to validate the selected algorithms in the selected configuration-frequency set (i.e., configuration 3 and frequency of 1.337 MHz) when varying electrode type.

1) Algorithm A: Volume estimation errors were represented as absolute values to facilitate the general comparison of electrode performance (see Fig. 5).

Considering naked bladders filled with standard saline solution (red lines), volume estimation errors significantly decreased with increasing filling volume. In particular, volume estimation errors (average error ± standard deviation%) ranged from 53.17 ± 1% (50 mL) to 13.54 ± 15.86% (250 mL) for the patch electrodes. On the other hand, needle electrodes generally featured higher errors but comparable standard deviations, especially for lower volumes. Volume estimation errors varied between 99.12 ± 1% (50 mL) and 19.51 ± 14.39% (250 mL). The high estimation errors in the low volume range (below 150 mL) observed for needle electrodes could be a consequence of the displacement the needles undergo in the first filling phase during which abrupt changes in bladder shape were observed (i.e., the tissue under the electrodes stretched and thinned).

TABLE II

r^2 AND RMSE (cm) VALUES OF THE FITTING METHODS USED TO ESTIMATE THE INTER-ELECTRODE DISTANCES FROM $\Delta R_{\text{BLADDER}}$ AND $\Delta X_{\text{BLADDER}}$ (ALGORITHM B) ARE REPORTED FOR THE TWO SELECTED CONFIGURATIONS, FOR BOTH ELECTRODE TYPES. RESULTS FOR DIFFERENT POLYNOMIAL DEGREES ARE REPORTED (1–2–5)

ALGORITHM B						
PATCH ELECTRODES						
	CONFIGURATION 3			**CONFIGURATION 5**		
Statistical Parameter	**r^2**	**RMSE (cm)**		**r^2**	**RMSE (cm)**	
Polynomial Order	**1**	**2**	**5**	**1**	**2**	**5**
$\Delta R_{\text{bladder}}$ - d_{measured}	0.20	0.90	0.90	0.29	1.33	1.29
$\Delta X_{\text{bladder}}$ - d_{measured}	0.17	0.90	0.90	0.22	1.35	1.30
$\Delta R_{\text{bladder}}$ - $\Delta X_{\text{bladder}}$ - d_{measured}	0.21	0.90	0.91	0.31	1.36	1.32
NEEDLE ELECTRODES						
	CONFIGURATION 3			**CONFIGURATION 5**		
Statistical Parameter	**r^2**	**RMSE (cm)**		**r^2**	**RMSE (cm)**	
Polynomial Order	**1**	**2**	**5**	**1**	**2**	**5**
$\Delta R_{\text{bladder}}$ - d_{measured}	0.12	0.76	0.75	0.09	1.32	1.31
$\Delta X_{\text{bladder}}$ - d_{measured}	0.01	0.84	0.81	0.17	1.27	1.23
$\Delta R_{\text{bladder}}$ – $\Delta X_{\text{bladder}}$ - d_{measured}	0.14	0.78	0.80	0.19	1.23	1.16

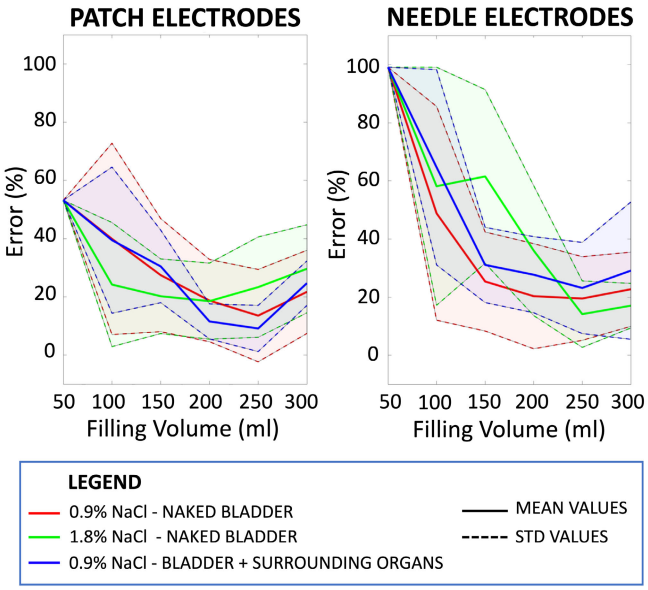

Fig. 5. Performance of Algorithm A in terms of absolute percentage (mean and standard deviations) errors of volume estimations are reported for both types of electrodes. The errors of the three experimental conditions are compared.

For both electrode types, there was an increase in the percentage error for volumes greater than 250 mL. When the bladder was full (300 mL), estimation errors of 21.71 ± 14.28% and 22.71 ± 12.77% were achieved for patch and needle electrodes, respectively. From these results, it was clear that the two types of electrodes had similar performances for volumes greater than 150 mL. Indeed, the decrease in bladder wall thickness with increasing volumes caused a reduction of Z_{wall} contribution [see Fig. 1(a)], thus a reduction in estimation errors (i.e., R_{urine} was the main contributor).

For Algorithm A, when increasing the ion concentration (from 0.9% to 1.8%, green lines in Fig. 5), the contribution of the bladder tissue (Z_{wall}) remained the same as in the previous condition. However, an increase in the ions in the

injected solution involved a significant variation in its electrical properties, thus a significant decrease in R_{urine}. As a consequence, higher estimation errors were observed for volumes above 200 mL since the impedance measures deviated from the fit polynomial. In fact, even if patch electrodes showed better performances for lower volumes (an average decrease of 5.78% in the estimation errors from 50 to 200 mL), an average increase of 8.86% in the estimation errors was observed for volumes higher than 200 mL.

On the other hand, a significant worsening in performance was reported for needle electrodes, with much higher estimation errors (average increase of 12.03%) and higher standard deviations (average increase of 3.90%), especially for volumes below 250 mL.

On the contrary, by placing tissues to simulate the organs around the bladder (blue lines in Fig. 5), we added a new impedance contribution (in parallel with Z_{bladder}). By considering adding the same quantity of simulated organs throughout all tests, the final contribution of the tissues was defined as $Z_{\text{bladder}} + Z_{\text{organs}}$, in which the overall contribution of the bladder wall (and consequent biological variability) was decreased. In this sense, we observed lower standard deviations along the entire range of volumes for both types of electrodes (average decrease of 6.23% and 4.07% for patch and needle electrodes, respectively) and similar estimation errors (slight average increase in estimation errors of 6.49% for needle electrodes).

2) Algorithm B: The filling volumes of the bladder ($V_{\text{estimated}}$) were obtained with the geometric formula for sphere volume (see Fig. 4) and the absolute average percentage errors (considering V_{injected} and $V_{\text{estimated}}$) are reported in Fig. 6.

Considering the standard experimental conditions (red lines in Fig. 6), a decrease in the absolute percentage estimation errors and standard deviations with increasing volume was observed for volumes below 200 mL for both electrode types. In particular, absolute errors ranging from 50.45 ± 22.04% (100 mL) to 12.31 ± 9.88% (200 mL) for patch electrodes, and from 70.14 ± 21.58% (100 mL) to 6.14 ± 8.60% (200 mL) for needle electrodes were reported. At low filling volumes (50 mL), the major absolute estimation errors were observed as a consequence of the sphere approximation of the bladder as still presenting an almost collapsed shape for low filling volumes. In addition, it was observed that the shape of the bladder could be approximated to a sphere for volumes below 200 mL, but tended to diverge from it for greater volumes reaching percentage errors of 33.17 ± 11.61% (patch electrodes) and 38.82 ± 5.54% (needle electrodes) at 300 mL.

For Algorithm B, even with increased ion concentration (green lines in Fig. 6) and swine tissue placed around the bladder to simulate adjacent organs (blue lines in Fig. 6), the behavior remained the same as in standard conditions. In the first case, an average increase in errors of 0.96% (patch electrodes) and 1.36% (needle electrodes) with a corresponding decrease in standard deviations of 4.55% (patch electrodes) and 2.22% (needle electrodes) was observed along the entire range of volumes. In the second case, an average increase in the estimation errors of 3.84% and 6.06% (with an average decrease in standard deviations of 5.33% and 2.14%) were reported for patch and needle electrodes, respectively.

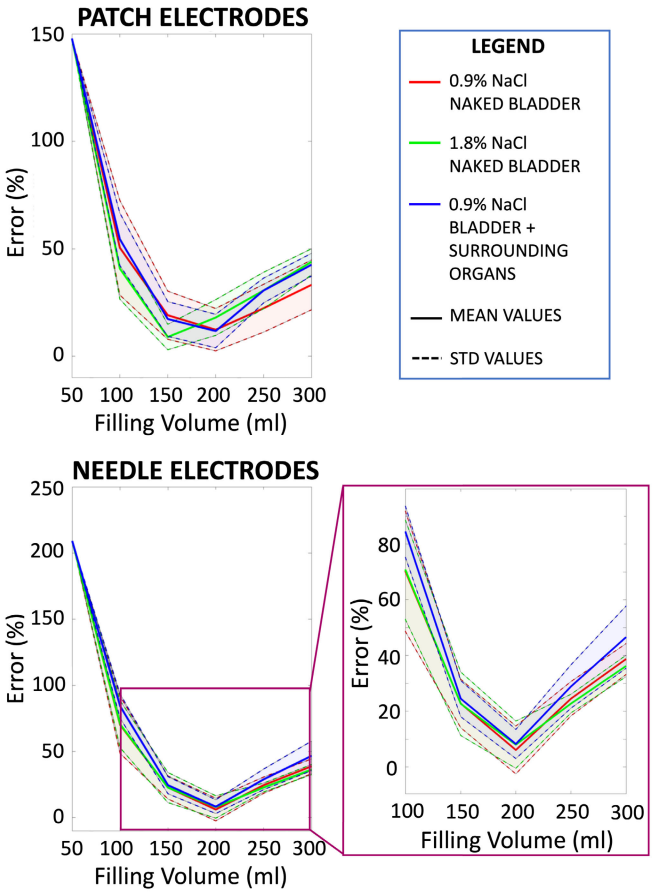

Fig. 6. Performance of Algorithm B in terms of absolute percentage (mean and standard deviations) errors of volume estimations are reported for both types of electrodes. The errors of the three experimental conditions are compared.

D. Comparison of the Volume Estimation Algorithms

To better compare the performances of the two tested algorithms (Algorithms A and B), we analyzed estimation errors not as absolute values. This allowed us to study whether over- or underestimation of bladder volume occurred (see Fig. 7). In this sense, it was observed a tendency to overestimate volumes below 150 mL and underestimate the larger ones, for both the algorithms. In all the conditions tested, both algorithms proved unable to recognize volumes at the two extremes of the range (around 50 and 300 mL). The spherical approximation reinforces this tendency for the second algorithm as the sphere does not approximate well the bladder for low (bladder still collapsed) and high filling volumes (bladder enlarges and diverges from the spherical shape). In fact, the natural bladder had a tendency to open in an anisotropic manner due to gravity, which affects the direction of urine accumulation, and due to the elasticity of the tissue in the different areas of the bladder (bladder neck and dome). Therefore, in the sphere approximation, the accumulations of liquids that involve a deformation of the bladder were not considered.

In addition, the diameter of the sphere was derived assuming the angle between the electrodes was known. This assumption combined with the manual twine thread positioning connecting the electrodes centers, surely contributed to the estimation error. The estimation errors were obtained by the superposition of three contributions: the errors made in estimating the

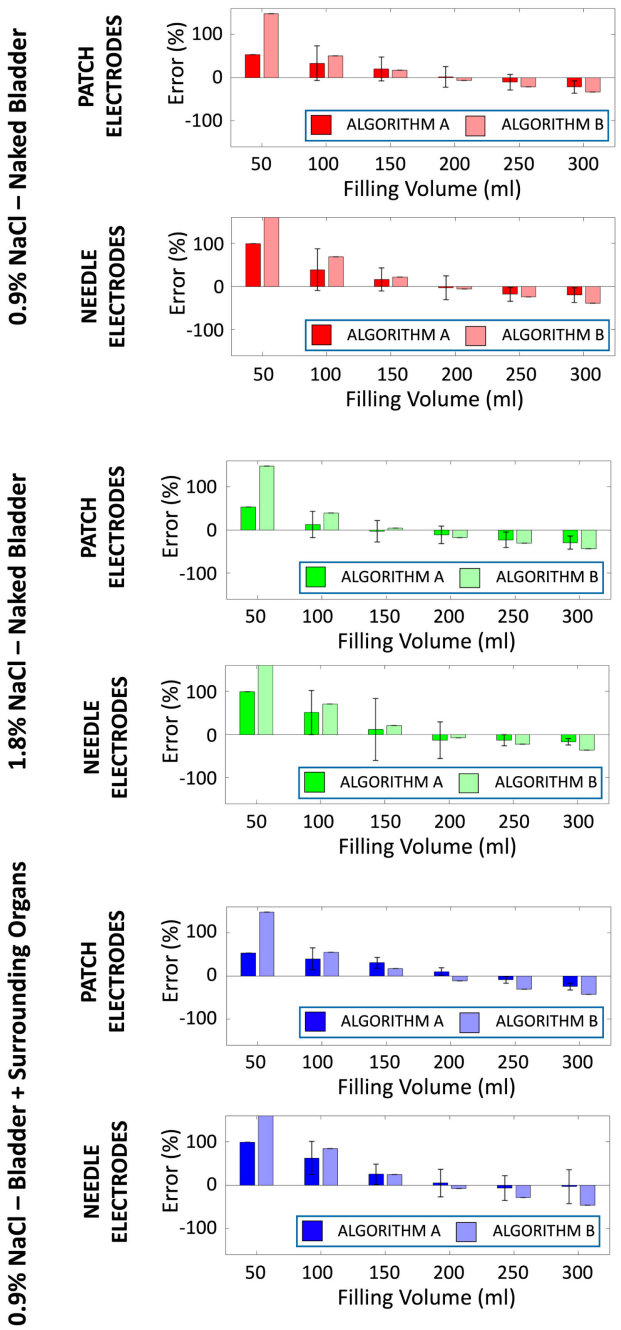

Fig. 7. Performances of both algorithms in terms of percentage errors (mean and standard deviations) with the sign of volume estimations are reported for both types of electrodes. The errors of the three experimental conditions are compared.

inter-electrode distance starting from the impedance components, the errors made in positioning the twine thread, and the errors made in approximating the bladder shape to a sphere. Although Algorithm B featured lower standard deviations and more similar performances in all the experimental conditions tested, the first algorithm had significantly lower errors for both electrode types.

E. Comparison of Ex Vivo and In Vivo Performances

The $\Delta R_{\text{bladder}}$ and $\Delta X_{\text{bladder}}$ collected during both ex vivo and in vivo filling tests are reported in Fig. 8. For both components of impedance, the same data trend is observed

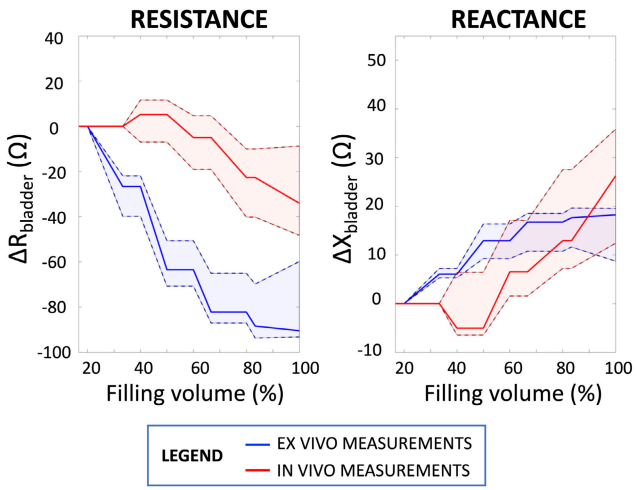

Fig. 8. $\Delta R_{\text{bladder}}$ and $\Delta X_{\text{bladder}}$ during bladder filling for the selected electrode configuration and working frequency, and using the selected electrode type. The data are reported for ex vivo (in blue) and in vivo (in red) tests.

during bladder filling between ex vivo (in blue) and in vivo (in red) tests. In this sense, a decrease in resistance and an increase in reactance with increasing volume are clearly visible.

$\Delta R_{\text{bladder}}$ and $\Delta X_{\text{bladder}}$ measures have been provided as input to the selected Algorithm A for volume estimation. As visible in Fig. 9, an average error of 29.36% was obtained for volumes above 40% of filling volume. In addition, in the in vivo environment, higher errors were recorded for low volumes, which decreased progressively up to half-fill volumes (minimum error of 10.04% at 60% of filling). Compared to ex vivo results, we obtained comparable average errors (considering the entire range of filling volumes) despite the greater variability of tissues surrounding the bladder in the in vivo setting. However, a double error of 42.85% was obtained at the bladder maximum capacity for in vivo tests as compared to ex vivo ones ($21.71 \pm 14.28\%$).

IV. Conclusion and Future Works

In this work, we introduced a new implantable sensing strategy based on bioimpedance sensors to restore urinary volume monitoring in patients with reduced or absent bladder sensation. Both ex vivo and in vivo tests demonstrated the feasibility of using commercial electrodes, patches, and needle types, for bioimpedance monitoring in the proposed application. The injected current frequency of 1.337 MHz featured wider dynamics of impedance over the tested volume range allowing us to better correlate the changes in impedance with increasing volumes. From the electrode configuration viewpoint, the vertical configuration with electrodes paired placed on the same face of the bladder at the level of the bladder neck and dome (configuration 3) allowed a monotonous trend of impedance components with increasing volume.

Two volume reconstruction algorithms were implemented, based on the direct correlation between bioimpedance readings and bladder volume (Algorithm A) or inter-electrode distance (with subsequent volume estimation by approximating the bladder shape to a sphere, Algorithm B). For both algorithms, a better fit of the bioimpedance measurements with the second-degree fitting polynomial was obtained. Algorithm

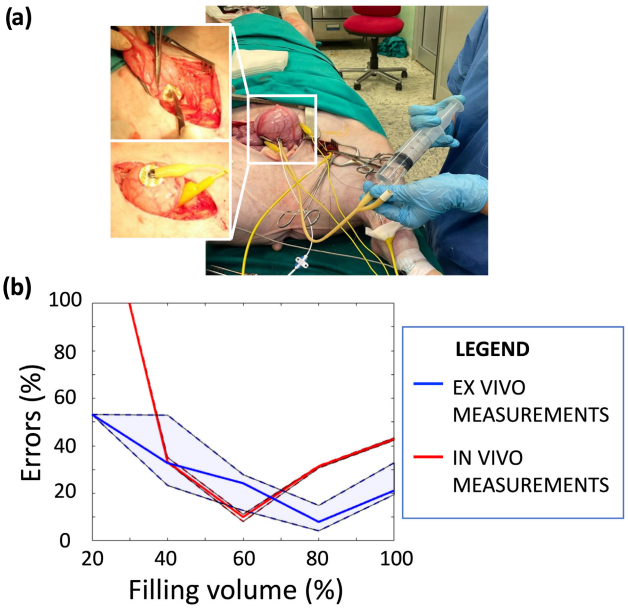

Fig. 9. In vivo impedance-based volume monitoring. (a) Implanted sensors and volume monitoring tests overview in vivo. (b) Performance of Algorithm A in terms of absolute percentage errors of volume estimations obtained for ex vivo (in blue) and in vivo (in red) tests.

A allowed to have lower estimation errors, especially for higher filling volumes (greater than 150 mL) with an average estimation error of 20.35% and 21.98% for patch and needle electrodes, respectively. The algorithm appeared to be influenced by variations in urine ion concentration with a worsening performance (especially for needle electrodes). However, estimation performance did not significantly vary in the presence of other tissues surrounding the bladder. On the other hand, Algorithm B appeared to be less affected by the experimental conditions and by inter-subject biological variability, presenting lower standard deviations. However, this algorithm is featured by significantly higher estimation errors being affected also by the geometrical approximation of the bladder shape.

From these observations, we selected Algorithm A and patch electrodes for the in vivo validation. The trend of resistance and reactance values was the same between ex vivo and in vivo tests, and in vivo we obtained comparable performance to the ex vivo one, with an average error of 29.36% for volumes above 40% of filling.

In the state-of-the-art, there are not many works on the monitoring of the bladder volume at a chronic and implantable level (see the Introduction section). Few strategies were proposed but not extensively tested in terms of monitoring performances, with most of the focus on the sensor itself. In addition, although several clinical and wearable bioimpedance-based solutions have been explored with promising results in monitoring bladder filling, there are not many quantitative studies to compare the results accomplished in this work. The use of patch electrodes attached to the external walls of the natural bladder to detect bioimpedance data seems promising since the errors obtained turn out to be acceptable (around 20% in the ex vivo setting–Algorithm A). These results proved only slightly worse than those obtained with external monitoring systems (e.g., based in the U.S., featuring estimation errors around 15% [21], [22]) or implantable artificial bladder systems equipped with magnetic field sensors (errors reached 12% but with highly controllable volume-geometry variations [23]). Larger errors were obtained when considering the in vivo setting, due to the presence of tissues with high conductivity surrounding the bladder. However, the great merit of these results is to accomplish comparable performances for the first time through implanted bioimpedance sensors suitable for natural bladder monitoring. Indeed, our final goal is to provide sensatory feedback to the patient with the aim of defining the right timing for urination. In this sense, providing a good estimate of urinary volume when approaching to bladder full-state is the key performance to be monitored and was successfully accomplished with the proposed strategy in the ex vivo setting. Preliminary results appear to be promising, and a better volume estimation can be achieved with a more accurate calibration of in vivo data.

Starting from the feasibility study presented in this work, future goals include the study and design of the electronics to complete the sensing system. To date, there are no miniaturized electronics to carry out our analysis at an implantable level; however, there are systems that could be taken as an example to be adapted for our application [24]. Furthermore, artificial detrusors could be coupled to the sensing proposed strategy to obtain a more complete system and to provide a solution even for patients with contractility dysfunctions of the detrusor muscle [25].

REFERENCES

[1] W. C. de Groat and N. Yoshimura, "Anatomy and physiology of the lower urinary tract," in *Handbook of Clinical Neurology*, vol. 130, D. B. Vodušek and F. Boller, Eds. Amsterdam, The Netherlands: Elsevier, 2015, pp. 61–108, doi: 10.1016/B978-0-444-63247-0.00005-5.

[2] Y. Aoki, H. W. Brown, L. Brubaker, J. N. Cornu, J. O. Daly, and R. Cartwright, "Urinary incontinence in women," *Nature Rev. Disease Primers*, vol. 3, no. 1, p. 17042, Jul. 2017, doi: 10.1038/nrdp.2017.42.

[3] D. E. Irwin, Z. S. Kopp, B. Agatep, I. Milsom, and P. Abrams, "Worldwide prevalence estimates of lower urinary tract symptoms, overactive bladder, urinary incontinence and bladder outlet obstruction," *BJU Int.*, vol. 108, no. 7, pp. 1132–1138, Oct. 2011, doi: 10.1111/j.1464-410X.2010.09993.x.

[4] F. Semproni, V. Iacovacci, and A. Menciassi, "Bladder monitoring systems: State of the art and future perspectives," *IEEE Access*, vol. 10, pp. 125626–125651, 2022, doi: 10.1109/ACCESS.2022.3221816.

[5] F. Semproni, M. Ibrahimi, I. Tamadon, V. Iacovacci, and A. Menciassi, "An innovative system based on bioimpedance measurements to define the bladder volume," Presented at the 47th ESAO Congr., 2021.

[6] S. Rodriguez, S. Ollmar, M. Waqar, and A. Rusu, "A batteryless sensor ASIC for implantable bio-impedance applications," *IEEE Trans. Biomed. Circuits Syst.*, vol. 10, no. 3, pp. 533–544, Jun. 2016, doi: 10.1109/TBCAS.2015.2456242.

[7] H. Cao et al., "An implantable, batteryless, and wireless capsule with integrated impedance and pH sensors for gastroesophageal reflux monitoring," *IEEE Trans. Biomed. Eng.*, vol. 59, no. 11, pp. 3131–3139, Nov. 2012, doi: 10.1109/TBME.2012.2214773.

[8] D. C. Walker, R. H. Smallwood, A. Keshtar, B. A. Wilkinson, F. C. Hamdy, and J. A. Lee, "Modelling the electrical properties of bladder tissue—Quantifying impedance changes due to inflammation and oedema," *Physiolog. Meas.*, vol. 26, no. 3, pp. 251–268, Jun. 2005, doi: 10.1088/0967-3334/26/3/010.

[9] A. Keshtkar, A. Keshtkar, and R. H. Smallwood, "Electrical impedance spectroscopy and the diagnosis of bladder pathology," *Physiolog. Meas.*, vol. 27, no. 7, pp. 585–596, Apr. 2006, doi: 10.1088/0967-3334/27/7/003.

[10] S. Hannah, P. Brige, A. Ravichandran, and M. Ramuz, "Conformable, stretchable sensor to record bladder wall stretch," *ACS Omega*, vol. 4, no. 1, p. 1, Jan. 2019, doi: 10.1021/acsomega.8b02609.

[11] M. Kim et al., "Polypyrrole/Agarose hydrogel-based bladder volume sensor with a resistor ladder structure," *Sensors*, vol. 18, no. 7, p. 2288, Jul. 2018, doi: 10.3390/s18072288.

[12] A. D. Mickle et al., "A wireless closed-loop system for optogenetic peripheral neuromodulation," *Nature*, vol. 565, no. 7739, pp. 361–365, Jan. 2019, doi: 10.1038/s41586-018-0823-6.
[13] V. Gaubert, H. Gidik, and V. Koncar, "Proposal of a lab bench for the unobtrusive monitoring of the bladder fullness with bioimpedance measurements," *Sensors*, vol. 20, no. 14, p. 3980, Jul. 2020, doi: 10.3390/s20143980.
[14] L. Yang et al., "Insight into the contact impedance between the electrode and the skin surface for electrophysical recordings," *ACS Omega*, vol. 7, no. 16, pp. 13906–13912, Apr. 2022, doi: 10.1021/acsomega.2c00282.
[15] T. Noguchi, S. Fukai, Y. Ishikawa, A. Shimizu, A. Kimoto, and I. Toyoda, "A urinary bladder volume measurement circuit using a simplified very small phase difference measurement circuit," *IEEJ Trans. Electron., Inf. Syst.*, vol. 137, no. 10, pp. 1304–1309, 2017, doi: 10.1541/ieejeiss.137.1304.
[16] R. Deanne. (1980). *Electrical Impedance of Human Urine*. University of Utah. Accessed: Jul. 29, 2021. [Online]. Available: https://collections.lib.utah.edu/details?id=190659
[17] R. Pewowaruk, D. Rutkowski, D. Hernando, B. B. Kumapayi, W. Bushman, and A. Roldán-Alzate, "A pilot study of bladder voiding with real-time MRI and computational fluid dynamics," *PLoS ONE*, vol. 15, no. 11, Nov. 2020, Art. no. e0238404, doi: 10.1371/journal.pone.0238404.
[18] T. Schlebusch et al., "Impedance ratio method for urine conductivity-invariant estimation of bladder volume," *J. Electr. Bioimpedance*, vol. 5, no. 1, pp. 48–54, Sep. 2014, doi: 10.5617/jeb.895.
[19] D. Miklavčič, N. Pavšelj, and F. X. Hart, "Electric properties of tissues," in *Wiley Encyclopedia of Biomedical Engineering*, M. Akay, Ed. Hoboken, NJ, USA: Wiley, 2006, Art. no. ebs0403, doi: 10.1002/9780471740360.ebs0403.
[20] R. J. Halter et al., "The correlation of in vivo and ex vivo tissue dielectric properties to validate electromagnetic breast imaging: Initial clinical experience," *Physiolog. Meas.*, vol. 30, no. 6, pp. S121–S136, Jun. 2009, doi: 10.1088/0967-3334/30/6/S08.
[21] *Bladderscan BVI 6100 Operation & Maintenance Manual PDF Download | ManualsLib*. Accessed: Nov. 22, 2021. [Online]. Available: https://www.manualslib.com/manual/1325394/Bladderscan-Bvi-6100.html
[22] Verathon Inc. *BladderScan Prime Plus*. Accessed: Nov. 18, 2021. [Online]. Available: https://www.verathon.com/bladderscan-prime-plus/
[23] S. Pane, T. Mazzocchi, V. Iacovacci, L. Ricotti, and A. Menciassi, "Smart implantable artificial bladder: An integrated design for organ replacement," *IEEE Trans. Biomed. Eng.*, vol. 68, no. 7, pp. 2088–2097, Jul. 2021, doi: 10.1109/TBME.2020.3023052.
[24] R. Bernasconi, D. Meroni, A. Aliverti, and L. Magagnin, "Fabrication of a bioimpedance sensor via inkjet printing and selective metallization," *IEEE Sensors J.*, vol. 20, no. 23, pp. 14024–14031, Dec. 2020, doi: 10.1109/JSEN.2020.3007619.
[25] G. Casagrande, M. Ibrahimi, F. Semproni, V. Iacovacci, and A. Menciassi, "Hydraulic detrusor for artificial bladder active voiding," *Soft Robot.*, vol. 10, no. 2, pp. 269–279, Apr. 2023, doi: 10.1089/soro.2021.0140.

Federica Semproni (Graduate Student Member, IEEE) received the B.S. and M.S. degrees in biomedical engineering from the Politecnico di Torino, Turin, Italy, in 2020. She is currently pursuing the Ph.D. degree in biorobotics with the Scuola Superiore Sant'Anna, Pisa, Italy.

In 2019, she joined the Motion Analysis Laboratory, Spaulding Rehabilitation Hospital (Harvard Medical School), Boston, MA, USA, as a Research Student. Her research interests include biomechatronic artificial organs, and novel active monitoring strategies for implantable medical devices.

Veronica Iacovacci (Member, IEEE) received the M.Sc. degree in biomedical engineering from the University of Pisa, Pisa, Italy, in 2013, and the Ph.D. degree in biorobotics from the Scuola Superiore Sant'Anna (SSSA), Pisa, in 2017.

She has been a Postdoctoral Fellow with SSSA and the Swiss Federal Institute of Technology and a Marie Curie Global Fellow jointly with SSSA and the Chinese University of Hong Kong, Hong Kong. She is currently a Tenure Track Assistant Professor of Bioengineering and Biomedical Robotics with SSSA. In the recent years, she has been focuses on microrobots imaging and retrieval, to bring these technologies closer to the clinical practice. Her research interests include microrobotics for medical applications with a focus on magnetic systems and implantable biorobotic organs.

Stefania Musco received the M.D. degree from Campus Biomedico University, Rome, Italy, in 2001, and the degree with specialization in urology from Tor Vergata University, Rome, in November 2006.

She is currently a Urologist Consultant with the Neurourology Department, Careggi University Hospital, Florence, Italy. Her main areas of interest are neuro-urology, urodynamics, diagnosis and treatment of female and male urinary incontinence, neuromodulation techniques including tibial, sacral, and pudendal.

Ms. Musco is a Secretary of the Italian Urodynamic Society, a Panel Member of the Neuro-Urology European Association Urology (EAU), and a Secretary of the International Neurourology Society (INUS).

Arianna Menciassi (Fellow, IEEE) received the M.Sc. degree in physics from the University of Pisa, Pisa, Italy, in 1995, and the Ph.D. degree in bioengineering from the Scuola Superiore Sant'Anna (SSSA), Pisa, in 1999.

She has been a Coordinator of the Ph.D. in BioRobotics since 2018 and she was appointed in 2019 as a Vice-Rector of SSSA. She is currently a Professor of Bioengineering and Biomedical Robotics with SSSA, where she is a Team Leader of the "Surgical Robotics and Allied Technologies," BioRobotics Institute. Her research interests include surgical robotics, microrobotics for biomedical applications, biomechatronic artificial organs, and smart and soft solutions for biomedical devices. She pays a special attention to the combination between traditional robotics, targeted therapy, and wireless solution for therapy (e.g., ultrasound- and magnetic-based).

Ms. Menciassi serves as an Editor for IEEE TRANSACTIONS ON ROBOTICS and the *APL Bioengineering*. She also serves in the Editorial Board of the *Soft Robotics Journal*.

Open Access funding provided by 'Scuola Superiore "S.Anna" di Studi Universitari e di Perfezionamento' within the CRUI CARE Agreement